J|A|C|S ARTICLES

Published on Web 11/09/2010

Iron Acyl Thiolato Carbonyls: Structural Models for the Active Site of the [Fe]-Hydrogenase (Hmd)

Aaron M. Royer,[†] Marco Salomone-Stagni,[‡] Thomas B. Rauchfuss,*[,†] and Wolfram Meyer-Klaucke*[,‡]

School of Chemical Sciences, University of Illinois at Urbana−Champaign, Urbana, Illinois 61801, United States, and EMBL Outstation c/o DESY, Notkestrasse 85, D-22603 Hamburg, Germany

Received August 19, 2010; E-mail: rauchfuz@uiuc.edu; wolfram@embl-hamburg.de

Abstract: Phosphine-modified thioester derivatives are shown to serve as efficient precursors to phosphine-stabilized ferrous acyl thiolato carbonyls, which replicate key structural features of the active site of the hydrogenase Hmd. The reaction of $Ph_2PC_6H_4C(O)SPh$ and sources of Fe(0) generates both $Fe(SPh)(Ph_2PC_6H_4CO)(CO)_3$ (**1**) and the *di*ferrous diacyl $Fe_2(SPh)_2(CO)_3(Ph_2PC_6H_4CO)_2$, which carbonylates to give **1**. For the extremely bulky arylthioester $Ph_2PC_6H_4C(O)SC_6H_3$-2,6-(2,4,6-trimethylphenyl)$_2$, oxidative addition is arrested and the Fe(0) adduct of the phosphine is obtained. Complex **1** reacts with cyanide to give $Et_4N[Fe(SPh)(Ph_2PC_6H_4CO)(CN)(CO)_2]$ (Et_4N[**2**]). ^{13}C and ^{31}P NMR spectra indicate that substitution is stereospecific and cis to P. The IR spectrum of [**2**]$^-$ in ν_{CN} and ν_{CO} regions very closely matches that for Hmd^{CN}. XANES and EXAFS measurements also indicate close structural and electronic similarity of Et_4N[**2**] to the active site of wild-type Hmd. Complex **1** also stereospecifically forms a derivative with $TsCH_2NC$, but the adduct is more labile than Et_4N[**2**]. Tricarbonyl **1** was found to reversibly protonate to give a thermally labile derivative, IR measurements of which indicate that the acyl and thiolate ligands are probably not protonated in Hmd.

Introduction

The conversion of carbon dioxide to methane is accomplished on a massive scale biologically, as indicated by the world's natural gas reserves (6254 trillion cubic feet).[1] The principal means by which microorganisms carry out this conversion has been delineated over the previous few decades.[2] This reduction involves a sequence of enzyme-catalyzed steps that utilize several unusual cofactors. For example, the biochemical cycle starts with the conversion of CO_2 to a formamide using a methanofuran cofactor and ends with the hydrogenolysis of a CH_3-S bond in coenzyme M. As a source on new ideas on catalysis, this collection of cofactors represent potentially rewarding targets. The biosynthesis and mode of action are areas ripe for discovery, and perhaps applications.

The most recently elucidated step in the archaeal methanogenic cycle is the reduction of a stabilized carbocation to the corresponding methylene derivative.[3] Normally, this conversion is effected by a [NiFe]-hydrogenase in the hydrogenotrophic methanogens, but under conditions where nickel is insufficiently bioavailable, the organism up-regulates backup enzymes that catalyze the same conversion.[4] These enzymes are called H_2-forming methylenetetrahydromethanopterin dehydrogenase (Hmd, PDB 3F47) and F_{420}-dependent methylene tetrahydromethanopterin dehydrogenase (Mtd, PDB 3IQF). Hmd was originally thought to be free of metals because catalysis was found initially to be insensitive to the presence of CO. Later work showed that Hmd requires iron and is inhibited by CO.[5] Over the course of the preceding five years, the structure of the active site has been elucidated using both the native protein as well as mutants.[6−10] The protein harbors an active site consisting of the third example of a iron thiolato carbonyl center found in biology.[11,12] The fact that these species catalyze reactions involving H_2 is an example of convergent evolution and an indicator of the deep significance of the Fe-SR-CO system.[11]

The environment of the Fe center in Hmd is Fe(SR)(acyl)L$(CO)_2$X, where L is an N-bonded ligand that is a derivative

[†] University of Illinois at Urbana−Champaign.
[‡] EMBL Outstation.

(1) Energy Information Administration. World Proved Reserves of Oil and Natural Gas, Most Recent Estimates, http://www.eia.doe.gov/emeu/international/reserves.html, March 3, 2009.
(2) Thauer, R. K. *Microbiology* **1998**, *144*, 2377–2406.
(3) Shima, S.; Thauer, R. K. *Chem. Rec.* **2007**, *7*, 37–46.
(4) Afting, C.; Hochheimer, A.; Thauer, R. K. *Arch. Microbiol.* **1998**, *169*, 206–210. Afting, C.; Kremmer, E.; Brucker, C.; A., H.; Thauer, R. K. *Arch. Microbiol.* **2000**, *174*, 225–232.
(5) Lyon, E. J.; Shima, S.; Buurman, G.; Chowdhuri, S.; Batschauer, A.; Steinbach, K.; Thauer, R. K. *Eur. J. Biochem.* **2004**, *271*, 195–204.
(6) Shima, S.; Pilak, O.; Vogt, S.; Schick, M.; Stagni, M. S.; Meyer-Klaucke, W.; Warkentin, E.; Thauer, R. K.; Ermler, U. *Science* **2008**, *321*, 572–575.
(7) Hiromoto, T.; Ataka, K.; Pilak, O.; Vogt, S.; Stagni, M. S.; Meyer-Klaucke, W.; Warkentin, E.; Thauer, R. K.; Shima, S.; Ermler, U. *FEBS Lett.* **2009**, *583*, 585–590.
(8) Hiromoto, T.; Warkentin, E.; Moll, J.; Ermler, U.; Shima, S. *Angew. Chem., Int. Ed.* **2009**, *48*, 6457–6460.
(9) Lyon, E. J.; Shima, S.; Boecher, R.; Thauer, R. K.; Grevels, F.-W.; Bill, E.; Roseboom, W.; Albracht, S. P. J. *J. Am. Chem. Soc.* **2004**, *126*, 14239–14248.
(10) Korbas, M.; Vogt, S.; Meyer-Klaucke, W.; Bill, E.; Lyon, E. J.; Thauer, R. K.; Shima, S. *J. Biol. Chem.* **2006**, *281*, 30804–30813.
(11) Armstrong, F. A.; Fontecilla-Camps, J. C. *Science* **2008**, *321*, 498–499.
(12) Heinekey, D. M. *J. Organomet. Chem.* **2009**, *694*, 2671–2680.

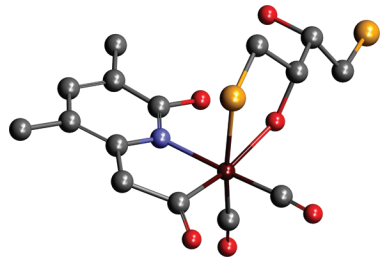

Figure 1. Structure of the active site of the jHmd C176A mutant with dithiothreitol (DTT) replacing cys176 (PDB 3H65) (*Methanococcus jannaschii*).[7] One OH of the DTT occupies the site trans to acyl. Color scheme: brown, Fe; blue, N; red, O; purple, P; yellow, S; gray, C.

of either 2-hydroxypyridine or 2-pyridonate and X occupies an apparently labile site. In the crystal structure X has been modeled as oxygen (e.g., of water),[7] which is in line with the EXAFS analysis.[13] In the mutant protein, the oxygenic ligand is provided by an alcohol (Figure 1). Inhibited forms of the protein have been prepared where X is cyanide and CO. The cyanide derivative Hmd^{CN} is stable, but its formation reverses at high dilution, whereas the CO-inhibited form Hmd^{CO} is highly labile, in accord with the weak inhibiting effect of this ligand.[3] These inhibited forms, especially Hmd^{CO} and Hmd^{CN}, represent suitable synthetic targets, since they are coordinatively saturated. Furthermore, models for Hmd^{CO} could serve as precursors to catalytically active states.

From the structural perspective, the presence of the acyl ligand is striking. Fe-acyls are common in synthetic organometallic chemistry,[14] for example, $(C_5H_5)(CO)_2FeC(O)Me$ and $[(CO)_4FeC(O)Me]^-$, but are unusual in biology. Acyl nickel intermediates have been invoked in acetogenesis,[15] which is catalyzed by the enzyme acetyl Co-A synthase.[16] In Hmd, the acyl ligand may function as a trans directing group, stereoselectively labilizing the site that binds H_2. Normally, acyl ligands are cis labilizing because of the facility of the η^1- to η^2-acyl conversion,[17] but if constrained in a chelate ring as in Hmd's active site, then we speculate that an acyl can exert a trans influence comparable to that of an aryl group.[18]

For first-generation models of Hmd, we sought to incorporate the most distinctive ligand, the acyl. Prior to our work, acyl thiolato *mono*iron complexes were unknown, although *di*iron complexes of the type $Fe_2(SR)(acyl)(CO)_6$ had been described. Specifically, Seyferth and co-workers prepared a series of diiron acyl thiolates via the oxidative addition of alkyl and arythioesters to Fe(0) reagents (eq 1).[19] The results presented in this paper

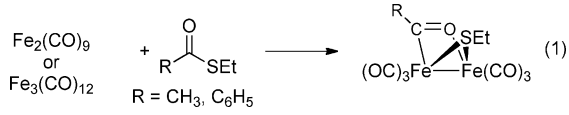

suggest that these diiron compounds arise via monoiron acylthiolate complexes. The oxidative addition of thioesters has also been described for complexes of Rh(I)[20] and Pt(0)[21] and is of continuing interest for applications in organic synthesis.[22,23] Thioester−iron interactions have been implicated in transformations relevant to the origin of life.[24]

We had previously described the oxidative addition of thioester-modified phosphines to Fe(0) reagents to give diiron μ-thiolato species of the type $Fe_2(SPh)_2(Ph_2PC_6H_4CO)_2(CO)_3$.[25] This diferrous species carbonylates to afford the metastable monomer *fac*-$Fe(SPh)(Ph_2PC_6H_4CO)(CO)_3$ (**1**). This tricarbonyl was found to undergo monosubstitution to give derivatives mimicking other ligand-inhibited forms of Hmd, abbreviated Hmd^L. In our preliminary report, we had not crystallized monomeric models of known inhibited states, but this problem has now been solved. Herein we describe the structural characterization of **1** and its cyanide derivative, which constitute structural models for the active site of Hmd.

Following the discovery of the Fe−acyl bond in Hmd, several models have appeared. Hu and co-workers originally generated iron acyls stabilized by 2-mercaptopicoline derivatives.[26] More recently both the Hu and Pickett groups have developed acyl- or carbamoylpyridine derivatives of ferrous carbonyls.[27] The mechanism, including the role of the 2-pyridinol cofactor, has also attracted much interest from computational chemists.[28]

Results

Phosphine Thioesters. Thioester phosphines containing a variety of aryl and alkylthio substituents can be prepared via carbodiimide coupling of 2-diphenylphosphinobenzoic acid with a range of thiols (Scheme 1). The new compounds are air-stable pale yellow to colorless crystalline solids. Such thioesters have been previously investigated as peptide coupling reagents.[29] Isomeric thioesters of the type $Ph_2PC_6H_4SC(O)R$ are also known.[30]

Scheme 1

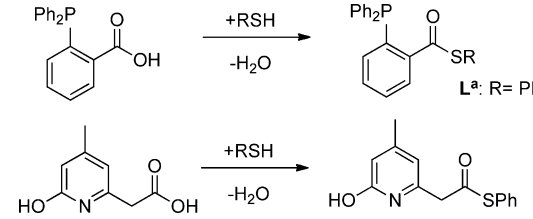

Fe(II) Acyl Thiolates. We found that several of the phosphine thioesters react with iron carbonyls to afford iron(II) acyl thiolato derivatives. A useful iron(0) source was Fe(bda)$(CO)_3$ (bda =

(13) Salomone-Stagni, M.; Stellato, F.; Whaley, C. M.; Vogt, S.; Morante, S.; Shima, S.; Rauchfuss, T. B.; Meyer-Klaucke, W. *Dalton Trans.* **2010**, *39*, 3057–3064.
(14) Plietker, B., Ed. *Iron Catalysis in Organic Chemistry*; Wiley-VCH: Weinheim, 2008.
(15) Tucci, G. C.; Holm, R. H. *J. Am. Chem. Soc.* **1995**, *117*, 6489–6496.
(16) Lindahl, P. A.; Graham, D. E. *Met. Ions Life Sci.* **2007**, *2*, 357–415. Fontecilla-Camps, J. C.; Amara, P.; Cavazza, C.; Nicolet, Y.; Volbeda, A. *Nature* **2009**, *460*, 814–822.
(17) Ford, P. C.; Rokicki, A. *Adv. Organometal. Chem.* **1988**, *28*, 139–206.
(18) Hartwig, J. F. *Organotransition Metal Chemistry, from Bonding to Catalysis*; University Science Books: New York, 2010.
(19) Seyferth, D.; Womack, G. B.; Archer, C. M.; Dewan, J. C. *Organometallics* **1989**, *8*, 430–442.
(20) Shaver, A.; Uhm, H. L.; Singleton, E.; Liles, D. C. *Inorg. Chem.* **1989**, *28*, 847–851.
(21) Minami, Y.; Kato, T.; Kuniyasu, H.; Terao, J.; Kambe, N. *Organometallics* **2006**, *25*, 2949–2959.
(22) Tokuyama, H.; Yokoshima, S.; Yamashita, T.; Lin, S.-C.; Li, L.; Fukuyama, T. *J. Braz. Chem. Soc.* **1998**, *9*, 381–387. Fukuyama, T.; Lin, S.-C.; Li, L. *J. Am. Chem. Soc.* **1990**, *112*, 7050–7051. Mori, Y.; Seki, M. *Org. Synth.* **2007**, *84*, 285–294. Liebeskind, L. S.; Srogl, J. *J. Am. Chem. Soc.* **2000**, *122*, 11260–11261.
(23) Looman, S. D.; Giese, S.; Arif, A. M.; Richmond, T. G. *Polyhedron* **1996**, *15*, 2809–2811.
(24) Huber, C.; Wächtershäuser, G. *Science* **1997**, *276*, 245–247. Wächtershäuser, G. *Philos. Trans R. Soc.* **2006**, *361*, 1787–1806.
(25) Royer, A. M.; Rauchfuss, T. B.; Gray, D. L. *Organometallics* **2009**, *28*, 3618–3620.
(26) Chen, D.; Scopelliti, R.; Hu, X. *J. Am. Chem. Soc.* **2009**, *132*, 928–929.

Scheme 2. Isomers Proposed for $Fe_2(SPh)_2(Ph_2PC_6H_4CO)_2(CO)_3$

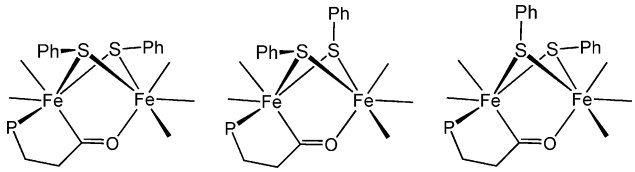

benzylideneacetone), but $Fe_2(CO)_9$ was also effective. Spectroscopic analysis of the reaction of $Ph_2PC_6H_4$-2-C(O)SPh (**L**[a]) with the highly labile cyclooctene complex $Fe(CO)_3(C_8H_{14})_2$[31] indicated displacement of only one cyclooctene ligand to give a monophosphine adduct. Thioesters derived from EtSH and *tert*-BuSH gave diiron compounds that were spectroscopically similar to the PhS derivative (see below), but these alkylthiolato diiron compounds resisted carbonylation to the monoiron complexes (see below).

The simple thioester **L**[a] gave the cleanest and highest yielding reaction and became the main focus for our efforts. Treatment of a hot THF suspension of $Fe_2(CO)_9$ with **L**[a] was found to give diiron dithiolato complexes with the formula $Fe_2(SPh)_2(CO)_3[Ph_2PC_6H_4C(O)]_2$ (eq 2).[25]

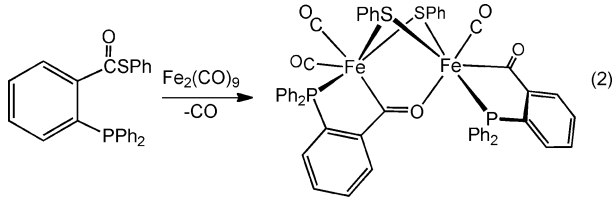

(2)

This diiron species exists as a mixture of isomers that are proposed to differ with respect to the orientation of the μ-SPh groups (Scheme 2).[32] Other aryl thioesters (Ar = C_6H_4-2-OMe, 2,4,6-$^iPr_3C_6H_2$) also gave derivatives of the type $Fe_2(SAr)_2(Ph_2PC_6H_4CO)_2(CO)_3$, but these conversions were less efficient. Using an extremely bulky arylthioester, we were able to arrest the oxidative addition. Thus, treatment of $Fe_2(CO)_9$ with $Ph_2PC_6H_4C(O)SC_6H_4$-2,6-(Ar*)$_2$ (Ar* = 2,4,6-trimethylphenyl) gave the monophosphine adduct of $Fe(CO)_4$. The IR spectrum of this product matches that for known derivatives of the type $Fe(CO)_4(PR_3)$.[33]

Thioester Derivatives of Nitrogen-Based Heterocycles. We also examined the reaction of thioester-functionalized *N*-heterocycles with Fe(0) reagents (see Scheme 1). The thiophenolate esters of quinoline-8-carboxylic acid[20] and 2-hydroxy-4-methylpyridine-6-acetic acid were synthesized by the usual coupling methods (Scheme 1). Both derivatives were reactive toward $Fe_2(CO)_9$ and (bda)$Fe(CO)_3$, but $Fe_2(SPh)_2(CO)_6$ was the only Fe carbonyl product detected.

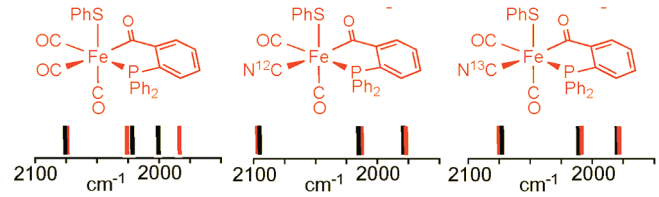

Figure 2. Energies of ν_{CN} and ν_{CO} for selected model compounds and Hmd[CO] and Hmd[CN].

Table 1. Selected IR Data for Model Compounds and for Hmd from *M. marburgensis*[9]

sample[a]	ν_{CO} (cm^{-1})
Hmd[CO] from *M. marburgensis*[9]	2074, 2020, 1981
$Fe(SPh)(Ph_2PC_6H_4CO)(CO)_3$ (**1**)	2075, 2025, 2001
(1:1 CH_2Cl_2:MeOH)	(2077, 2028, 2005)
Hmd[CN] from *M. marburgensis*[9]	2090 (ν_{CN}), 2020, 1956
Et_4N[$Fe(SPh)(Ph_2PC_6H_4CO)(CN)(CO)_2$] ($Et_4N$[**2**])	2093 (ν_{CN}), 2013, 1954
(1:1 CH_2Cl_2:MeOH)	(2093 (br, ν_{CN}), 2026, 1973)
Et_4N[$Fe(SPh)(Ph_2PC_6H_4CO)(^{13}CN)(CO)_2$]	2050 (ν_{CN}), 2012, 1954
$Fe(SPh)(Ph_2PC_6H_4CO)(CNCH_2Ts)(CO)_2$	2154 (ν_{CN}), 2042, 1988

[a] Models in CH_2Cl_2 solution unless otherwise indicated; enzyme in aqueous solution.

$Fe(SPh)(Ph_2PC_6H_4CO)(CO)_3$. Compound **1** was obtained by high-pressure carbonylation of a warm solution of the aforementioned diiron derivative. Solutions of the monomer **1** were found to decarbonylate at room temperature, returning to the diiron complex, but solutions of **1** were stable for days at < −10 °C. Crystalline samples of **1** proved stable at room temperature in air for weeks. Exposure of a solution of complex **1** to 1 atm of ^{13}CO at room temperature resulted in rapid (<5 min) exchange of all sites to give $Fe(SPh)(Ph_2PC_6H_4CO)(^{13}CO)_3$. The ^{31}P NMR spectrum of this species confirmed the arrangement of the CO ligands, since three separate $^{13}C-^{31}P$ couplings are observed with J = 58, 21, and 16 Hz. In $Fe(CO)_3(PMe_3)(\eta^2$-$Me_3SiCCSiMe_3)$, the $^{13}CO-^{31}P$ coupling constants are 59 (trans) and 35 Hz (cis).[34]

[$Fe(SPh)(Ph_2PC_6H_4CO)(CN)(CO)_2$]$^-$. Complex **1** reacts smoothly with cyanide to afford the anion [$Fe(SPh)(Ph_2PC_6H_4CO)(CN)(CO)_2$]$^-$ ([**2**]$^-$), isolated as its Et_4N^+ salt. The ^{13}C and ^{31}P NMR spectra for Et_4N[**2**] and its ^{13}CN-labeled derivative indicate that substitution is stereospecific. The value of $J(^{31}P,^{13}C)$ indicates that cyanide is located cis to the phosphine ligand.[35] Unlike **1**, solutions of [**2**]$^-$ are stable with respect to loss of CO, as also seen for Hmd[CN].[9] The IR spectrum of [**2**]$^-$ in CH_2Cl_2 solution also closely matches the cyanide-inhibited form of Hmd, wherein cyanation also proceeds stereoselectively[9] (Figure 2, Table 1).

The cyanide derivative was further characterized by X-ray absorption spectroscopy. The XANES spectrum (Figure 3), indicative of the electronic structure of the iron site, closely matches that of the iron binding site in wild type mHmd[CN].[10] The intense pre-edge peak for the new complex is resolved as a doublet, assigned tentatively to the 1s−d/4p transition(s). [Note: The high resolution in the *K*-edge region was achieved with the Si(220) monochromator with an intrinsic resolution of 0.4 eV vs 0.9 eV for Si(111).] The XANES spectra for both

(27) Chen, D.; Scopelliti, R.; Hu, X. *Angew. Chem., Int. Ed.* **2010**, *49*, 7512–7515. Turrell, P. J.; Wright, J. A.; Peck, J. N. T.; Oganesyan, V. S.; Pickett, C. J. *Angew. Chem., Int. Ed.* **2010**, *49*, 7508–7511.
(28) Yang, X.; Hall, M. B. *J. Am. Chem. Soc.* **2009**, *131*, 10901–10908. Dey, A. *J. Am. Chem. Soc.* **2010**, *132*, 13892–13901. Stiebritz, M. T.; Reiher, M. *Inorg. Chem.* **2010**, *49*, 5818–5823.
(29) Myers, E. L.; Raines, R. T. *Angew. Chem., Int. Ed.* **2009**, *48*, 2359–2363.
(30) Zhang, J.; Wang, H.; Xian, M. *J. Am. Chem. Soc.* **2009**, *131*, 3854–3855.
(31) Fleckner, H.; Grevels, F. W.; Hess, D. *J. Am. Chem. Soc.* **1984**, *106*, 2027–2032.
(32) King, R. B. *J. Am. Chem. Soc.* **1962**, *84*, 2460.
(33) Conder, H. L.; Darensbourg, M. Y. *J. Organomet. Chem.* **1974**, *67*, 93–97.
(34) Dennett, J. N. L.; Ferguson, M. J.; McDonald, R.; Takats, J. *Can. J. Chem.* **2005**, *83*, 862–868.
(35) Rocchini, E.; Rigo, P.; Mezzetti, A.; Stephan, T.; Morris, R. H.; Lough, A. J.; Forde, C. E.; Fong, T. P.; Drouin, S. D. *J. Chem. Soc., Dalton Trans.* **2000**, 3591–3602.

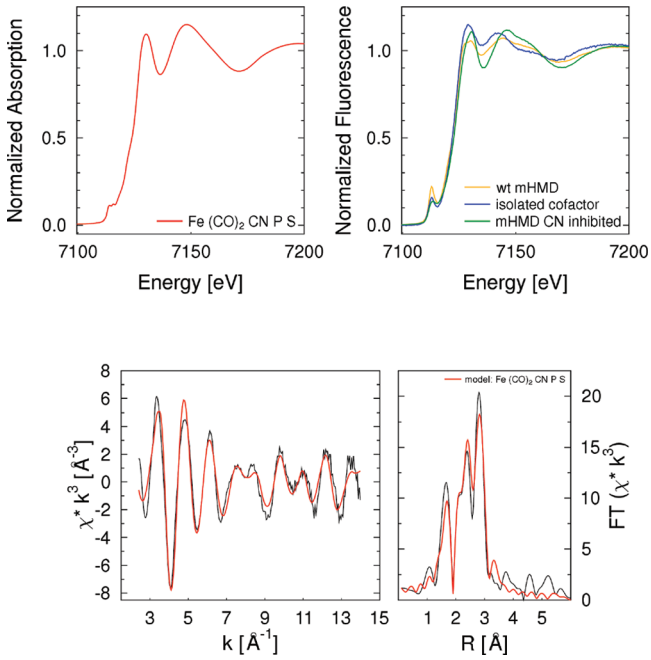

Figure 3. (Top) XANES spectrum of $Et_4N[Fe(SPh)(Ph_2PC_6H_4CO)(CN)(CO)_2]$ (left) and wild-type Hmd from *M. marburgensis*, the isolated Fe guanylyl-derived cofactor, as well as the cyanide-inhibited protein (right).[10] (Bottom) EXAFS spectrum and its Fourier transform with fits (red) for the model $Fe(CO)_3(CN)P(S)$ using the parameters in Table 2.

Table 2. Results of EXAFS Refinements for $Et_4N[Fe(SPh)(Ph_2PC_6H_4CO)(CN)(CO)_2]$ (Et_4N [**2**])[a]

ligand	*N*	*r* (Å)[b]	$2\sigma^2$ (Å^2)[b]
*C*O	2	1.81 ± 0.01	0.016 ± 0.003
C*O*	2	2.93 ± 0.01	0.012 ± 0.002[a]
*C*N	1	2.07 ± 0.03[c]	0.012 ± 0.004[b]
C*N*	1	3.19 ± 0.03	0.012 ± 0.002[a]
C	1	2.07 ± 0.03[c]	0.012 ± 0.004[b]
S	1	2.32 ± 0.02	0.008 ± 0.004
P	1	2.18 ± 0.06	0.02 ± 0.01

[a] Energy range, 10−750 eV; EF = −6.3 ± 0.3 eV; fit index, 0.954. [b] Indices a, b, and c indicate parameters that were refined jointly in order to lower the number of free parameters.

the CN-inhibited enzyme and Et_4N[**2**] show a mild shoulder in their rising edge, followed by a sharp resonance at about 7130 eV and a broad resonance at about 7150 eV. The position of the subsequent minimum at 7170 eV is mainly attributed to the distance of those ligands dominating the EXAFS pattern (Figure 3, Table 2). The high similarity of its position indicates strong similarities in the overall geometry of the active sites.

Adducts with $TsCH_2NC$. Reminiscent of its reactivity toward cyanide, complex **1** was found to undergo substitution by $TsCH_2NC$ under mild conditions. ^{31}P NMR spectroscopic measurements show that substitution occurs in seconds at about −10 °C. The formation of a single derivative (δ70.7 vs 72.5 for **1**; see Table 1 for ν_{CO} and ν_{CN}). The $TsCH_2NC$-substituted complex, **3**, is stable in solution at temperatures below −10 °C, but ^{31}P NMR measurements indicate that over the course of several minutes at −5 °C. The initial species converts to a mixture of three additional complexes, which are assumed to be isomers or the result of decarbonylation. At room temperature, this mixture simplifies over the course of a few minutes, as indicated by the appearance of two ^{31}P NMR signals in a 1:1 ratio, assigned to metastable diiron derivatives of the type $Fe_2(SPh)_2(Ph_2PC_6H_4CO)_2(CO)(RNC)_2$.

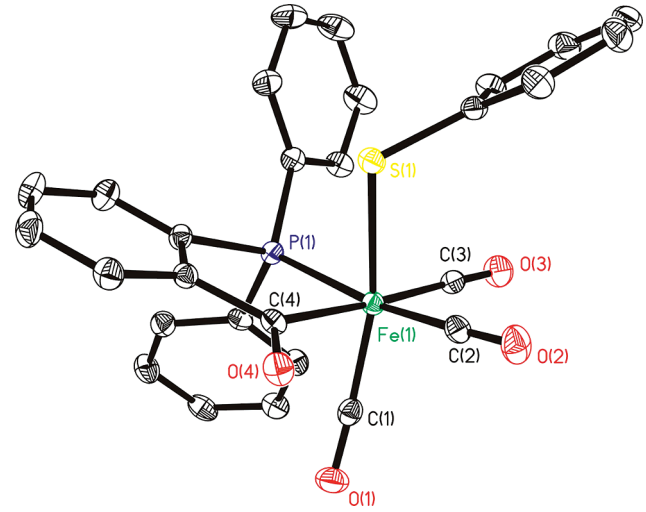

Figure 4. Structure of **1**, drawn with 35% probability ellipsoids. Hydrogen atoms were omitted for clarity.

Table 3. Selected Bond Lengths (Å) for **1** and $mHmd^{CO}$

bond	**1**	Hmd^{CO} *M. jannaschii*
Fe1−CO1	1.7844 (0.0018)	1.8260 (0.0081)
Fe1−CO2	1.8229 (0.0019)	1.8260 (0.0081)
Fe1−CO3	1.8395 (0.0018)	1.8260 (0.0081)
Fe1−C_{acyl}4	2.0202 (0.0016)	1.927 (0.044)
Fe1−N	–	2.0194 (0.076)
Fe1−S1	2.3457 (0.0005)	2.3162 (0.0056)

Protonation. Tricarbonyl **1** was found to undergo protonation at low temperatures to give unstable derivatives. In CH_2Cl_2 solution at −30 °C, protonation with $H(OEt_2)_2BAr^F_4$ (Ar^F = 3,5-$(CF_3)_2C_6H_3$) afforded a single product $[\mathbf{1}H]^+$, which lacks apparent hydride signals in its ^1H NMR spectrum. The IR spectrum (−26 °C) showed ν_{CO} bands (2090, 2041, and 2024 cm^{-1}), which are shifted by an average of 18 cm^{-1} to higher energies vs those for **1**. Addition of Et_3N to this cold solution of $[\mathbf{1}H]^+$ cleanly returned **1** (IR analysis). The IR data are thus consistent with protonation at a ligand, probably the thiolate[36] or the acyl group.[37] The corresponding *S*- and *O*-protonation of the ferrous thiolate $(C_5H_5)Fe(CO)_2SPh$ and the ferrous acyl $(C_5H_5)Fe(CO)(PPh_3)C(O)Me$ with HBF_4 and HBr, respectively, induces shifts in ν_{CO} by 40 and 32 cm^{-1}.[36,37] Upon warming its solution to 20 °C, $[\mathbf{1}H]^+$ was found to convert to a new product, which decomposed over the course of a few minutes.

Structure of $Fe(SPh)(Ph_2PC_6H_4CO)(CO)_3$. The tricarbonyl monomer **1** was further characterized by X-ray crystallography (Figure 4). The structure of **1** compares well with the recent structure of the C176A mutant of Hmd, which has been characterized at 2.15 Å resolution.[7] In this mutant, one cysteinyl ligand is replaced by one thiolate of dithiothreitol, which also provides an alcohol ligand in the coordination site trans to the acyl (see Figure 1). Selected bond lengths for **1** and $mHmd^{CO}$ and for **2** and $mHmd^{CN}$ are presented in Tables 3 and 4, respectively. The agreement between the bond lengths is excellent except for the Fe-acyl bond,[25,27] which for unknown reasons is 5-10% longer in models than in the protein.

Conclusions

Thioester derivatives of 2-diphenylphosphinobenzoic acid are versatile multifunctional reagents that enable easy access to phosphine-stabilized metal acyl thiolato carbonyls. The PhS

derivative was examined in detail and shown to adopt a structure very similar to the one modeled for the Fe site in Hmd^{CO}.[8] The major difference is the presence of the phosphine ligand vs the pyridyl group of the organic cofactor, but the phosphorus center offers the advantage of enabling ^{31}P NMR analysis of reaction mixtures. The pathway for the oxidative addition of the thioester to Fe(0) is illuminated by the finding that an extremely bulky phosphine thioester gave an adduct of the type $Fe(Ph_2PC_6H_4COSR)(CO)_4$. The isolation of this adduct is consistent with phosphine coordination preceding the chelate-assisted oxidative addition[38] of the thioester group. The oxidative addition of the thioester can then be envisioned to proceed via coordination of the thioether-like sulfur center[23] (eq 3). In contrast, oxidative addition of simple thioesters to Fe(0) reagents proceeds in low yields to give $[Fe(I)]_2$ derivatives of the type $Fe_2(SR)_2(CO)_6$ or $Fe_2(SR)(C(O)R')(CO)_6$.[19]

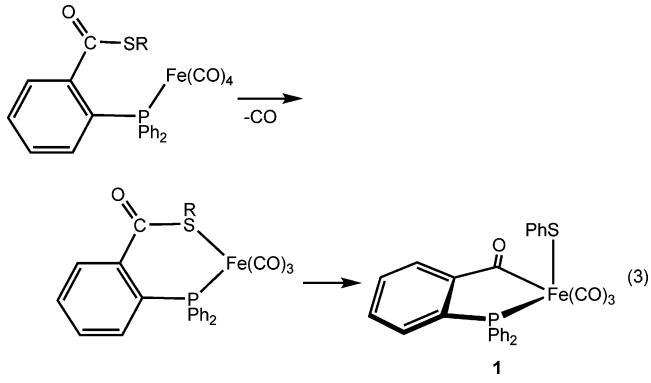

Whereas the phosphine facilitates oxidative addition of the thioester, the low affinity of Fe(0) for pyridines[39] prevented incorporation of the more biomimetic *N*-heterocyclic ligand on the $Fe(CO)_3$ center. Reactivity studies reinforce the electronic similarity between our model and the active site. Hmd stereoselectively binds ^{13}CO and CN^-.[9] ^{31}P NMR data show that **1** undergoes stereoselective substitution by both CN^- and $TsCH_2CN$, but CO is so labile in our model that stereoselective binding of ^{13}CO was not observed (eq 4). The lability of the site trans to acyl combined with the bridging tendency of thiolate ligands explains the facile conversion of **1** into the related $Fe_2(SR)_2$ derivative.[25] Our results suggest that the Fe-GP cofactor might be expected to degrade via dimerization.

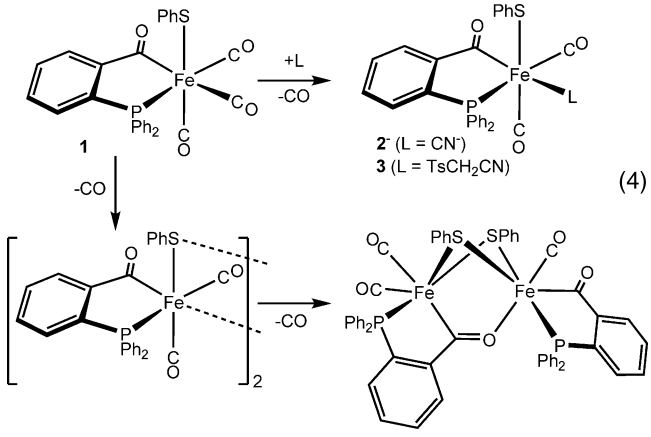

(4)

As indicated by comparisons of the XANES, EXAFS, and IR spectra for Hmd and Hmd^{CN} (*M. marburgensis*), $[Fe(SPh)(Ph_2PC_6H_4CO)(CN)(CO)_2]^-$ replicates the major details of both the electronic and geometric structure of the active site. This close match provides compelling evidence for the presence of a ferrous center in Hmd. The oxidation state of the Fe center in Hmd has been of recurring interest,[40] but the issue should now be considered settled in light of this and related modeling work on acyl-containing models.[26,27]

Table 4. Selected Bond Lengths (Å) for **2** and $mHmd^{CN}$

bond	**2**	Hmd^{CN} *M. jannaschii*
Fe1−CO1	1.81 ± 0.01	1.776 ± 0.006
Fe1−CO2	1.81 ± 0.01	1.776 ± 0.006
Fe1−CN3	2.07 ± 0.03	2.06 ± 0.01
Fe1−C_{acyl}4	2.07 ± 0.03	1.89 ± 0.01
Fe1−N	−	1.97 ± 0.01
Fe1−S1	2.32 ± 0.02	2.342 ± 0.006
Fe1−P1	2.18 ± 0.06	−

The present results highlight the anomalous effect of cyanide on the IR spectrum of Hmd. In Hmd^{CN}, two ν_{CO} bands are shifted to higher energies by 9 and 12 cm^{-1}. In this conversion, CN^- is assumed to displace a labile ligand such as water. Nonetheless, it is extremely rare that ν_{CO} bands shift to higher energy upon installing a cyanide ligand. For example, the average of the two ν_{CO} bands is 50 cm^{-1} *lower* in $[Fe(SPh)(Ph_2PC_6H_4CO)(CN)(CO)_2]^-$ than in $Fe(SPh)(Ph_2PC_6H_4CO)(CO)_3$.[9] One possible explanation for this anomaly is that CN^- affects the second coordination sphere of the ferrous center in Hmd, such as the protonation state of the pyridone ligand.

Our tricarbonyl model was also susceptible to reversible protonation, but only with strong acids. The ν_{CO} bands for the protonated tricarbonyl occur at 20−30 cm^{-1} above those seen for Hmd^{CO}. Furthermore, the protonated derivative is unstable at temperatures above −30 °C.

Experimental Section

General Considerations. Unless otherwise indicated, reactions were conducted using standard Schlenk techniques (N_2) at room temperature with stirring. All solvents were dried and degassed prior to use. Literature procedures afforded the following reagents: 2-diphenylphosphinobenzoic acid,[41] 2,6-dimesitylphenylthiol, 2,4,6-triisopropylthiol,[42] 2-hydroxy-4-methylpyridine-6-acetic acid,[43] $[H(Et_2O)_2]BAr^F{}_4$,[44] and $Fe(bda)(CO)_3$.[45] Benzenethiol, 2-methyl-2-propanethiol, ethanethiol, $TsCH_2NC$, and Et_4NCN were purchased from Sigma-Aldrich. DCC, 2-mercaptopyridine, and 4-dimethylaminopyridine were obtained from Fluka Analytical. EDAC (1-ethyl-3-(3-dimethylaminopropyl)carbodiimide hydrochloride) was

(36) McGuire, D. G.; Khan, M. A.; Ashby, M. T. *Inorg. Chem.* **2002**, *41*, 2202–2208.
(37) Green, M. L. H.; Hurley, C. R. *J. Organomet. Chem.* **1967**, *10*, 188–190.
(38) Landvatter, E. F.; Rauchfuss, T. B. *Organometallics* **1982**, *1*, 506.
(39) Boxhoorn, G.; Cerfontain, M. B.; Stufkens, D. J.; Oskam, A. *J. Chem. Soc., Dalton Trans.* **1980**, 1336–1341.
(40) Wang, X.; Li, Z.; Zeng, X.; Luo, Q.; Evans, D. J.; Pickett, C. J.; Liu, X. *Chem. Commun.* **2008**, 3555–3557. Guo, Y.; Wang, H.; Xiao, Y.; Vogt, S.; Thauer, R. K.; Shima, S.; Volkers, P. I.; Rauchfuss, T. B.; Pelmenschikov, V.; Case, D. A.; Alp, E. E.; Sturhahn, W.; Yoda, Y.; Cramer, S. P. *Inorg. Chem.* **2008**, *47*, 3969–3977.
(41) Hoots, J. E.; Rauchfuss, T. B.; Wrobleski, D. A. *Inorg. Synth.* **1982**, *21*, 175.
(42) Blower, P. J.; Bishop, P. T.; Dilworth, J. R.; Hsieh, T. C.; Hutchinson, J.; Nicholson, T.; Zubieta, J. *Inorg. Chim. Acta* **1985**, *101*, 63–65.
(43) Royer, A. M.; Rauchfuss, T. B.; Wilson, S. R. *Inorg. Chem.* **2008**, *47*, 395–397.
(44) Brookhart, M.; Grant, B.; Volpe, A. F. *Organometallics* **1992**, *11*, 3920–3922.
(45) Alcock, N. W.; Richards, C. J.; Thomas, S. E. *Organometallics* **1991**, *10*, 231–238.

purchased from Chem-Impex International. $MgSO_4$ and $NaHCO_3$ were purchased from Fisher Chemicals. $Fe_2(CO)_9$ was purchased from Strem Chemicals. Quinoline-8-carboxylic acid was purchased from Karl Industries. 2-Methoxythiophenol was obtained from SAFC Supply Solutions (St. Louis, MO). $K^{13}CN$ was purchased from Isotec. The silica gel used was 230−400 mesh Siliaflash P60 from Silicycle. Electrospray ionization mass spectra (ESI-MS) were acquired using a Micromass Quattro QHQ quadrupole−hexapole−quadrupole instrument. ^1H and ^{31}P NMR spectra were acquired on Varian UNITY INOVA TM 500NB and UNITY 500 NB instruments. Elemental analyses were performed by the School of Chemical Sciences Microanalysis Laboratory utilizing a model CE 440 CHN analyzer. In situ IR spectroscopic measurements were obtained using a ReactIR 4000 (Mettler-Toledo) instrument.

The preparation and purification of thioesters was found to be slightly less cumbersome utilizing the water-soluble reagent EDAC instead of DCC.

$Ph_2PC_6H_4$-2-C(O)SPh, L[a]. To a stirred solution of PhSH (870 μL, 8.475 mmol) in CH_2Cl_2 (20 mL) were added 2-diphenylphosphinobenzoic acid (2.36 g, 7.705 mmol) and DCC (1.75 g, 8.475 mmol). The reaction mixture was stirred 1 h, and the precipitated 1,3-dicyclohexylurea was filtered off. The yellow filtrate was concentrated under vacuum, and the residue was purified by column chromatography on silica gel, eluting with 50:1 hexane:ethyl acetate. The light yellow fraction was evaporated to give a crystalline solid that was dried under vacuum. Yield: 2.5 g (82%). ^{31}P NMR (202 MHz, CD_2Cl_2): δ −5.53. FDMS *m/z*: 398.2 (Calcd for M^+: 398.1). IR (CH_2Cl_2, cm^{-1}): ν_{CO} = 1677 (acyl). Anal. Calcd for $C_{25}H_{19}OPS$ (found): C, 75.36 (75.08); H, 4.81 (4.82); N, 0.00 (0.51).

$Ph_2PC_6H_4$-2-C(O)SC_6H_3-2,6-(C_6H_2-2,4,6-Me_3)$_2$. To a stirred solution of 2,6-dimesitylphenylthiol (1000 mg, 2.89 mmol) in CH_2Cl_2 (20 mL) were added 2-diphenylphosphinobenzoic acid (884 mg, 2.89 mmol), 4-dimethylaminopyridine (35 mg, 0.29 mmol), and EDAC·HCl (830 mg, 4.33 mmol) successively. The reaction solution was stirred for 3.5 h, and then washed three times with 1 N HCl (30 mL), followed by two times with saturated aqueous $NaHCO_3$ (30 mL), and once with water (30 mL). After drying over $MgSO_4$, the solution was evaporated. The residue was extracted into hexanes (8 mL) and precipitated a white solid within 15 min. The solid was collected by filtration, washed with 5 mL of hexanes, and dried under vacuum. Yield: 1.32 g (74%). ^1H NMR (500 MHz, CD_2Cl_2): δ 1.96 (s, 12H, mesityl-2,6-CH_3), 2.27 (s, 6H, mesityl-4-CH_3), 6.86 (s, 5H, aryl-H), 6.98−7.35 (15 H, aryl-H), 7.54 (t, 1H, aryl-H). ^{31}P NMR (202 MHz, CD_2Cl_2): δ −8.39. ESI-MS *m/z*: 635.6 (Calcd for MH^+: 635.3). IR (CH_2Cl_2, cm^{-1}): ν_{CO} = 1674 (acyl). Anal. Calcd for $C_{43}H_{39}OPS$ (found): C, 81.36 (80.89); H, 6.19 (6.32); N, 0.00 (0.46).

2-HO-4-Me-6-[CH_2C(O)SPh]-C_5H_2N. To a stirred solution of PhSH (61.4 μL, 0.5982 mmol) in THF (50 mL) were added 2-hydroxy-4-methylpyridine-6-acetic acid (100 mg, 0.5982 mmol) and DCC (123.4 mg, 0.5982 mmol) successively. The reaction mixture was stirred 4 days. Solvent was removed under vacuum, and CH_2Cl_2 (20 mL) was added. The precipitated 1,3-dicyclohexylurea was filtered off. The filtrate was concentrated under vacuum, and the yellow residue was washed with hexanes. The solid was extracted into ∼15 mL of EtOAc, and this extract was filtered through a ∼5-cm plug of silica gel. Solvent was removed by vacuum, and the residue was recrystallized from CH_2Cl_2 by the addition of hexanes, giving a white powder. Yield: 62 mg (40%). ^1H NMR (500 MHz, CD_2Cl_2): δ 2.23 (s, 3H, 4-CH_3), 3.89 (s, 2H, CH_2C(O)S) 6.15 (s, 1H, pyridyl-H), 6.34 (s, 1H, pyridyl-H), 7.43 (m, 5H, SC_6H_5). ESI-MS *m/z*: 260.3 (Calcd for MH^+: 260.1). IR (CH_2Cl_2, cm^{-1}): ν_{CO} = 1657 (acyl). Anal. Calcd for $C_{14}H_{13}NO_2S$ (found): C, 64.84 (64.96); H, 5.05 (5.61); N, 5.40 (6.14).

Fe($Ph_2PC_6H_4$C(O)SC_6H_3-2,6-Ar*$_2$)(CO)$_4$ (Ar* = 2,4,6-trimethylphenyl). A solution of $Ph_2PC_6H_4C(O)SC_6H_3$-2,6-Ar*$_2$ (94.2 mg, 0.148 mmol) in 20 mL of CH_2Cl_2 was transferred to a mixture 54 mg (0.148 mmol) of $Fe_2(CO)_9$ in 10 mL of CH_2Cl_2 at 0 °C. The mixture was stirred for 15 min and then allowed to warm to room temperature. The mixture was evaporated to dryness under vacuum, and the solid was rinsed with ∼15 mL of hexanes. The solid was recrystallized from 15 mL of Et_2O/30 mL of hexanes. Yield: 90 mg (76%). ^{31}P NMR (202 MHz, CD_2Cl_2): δ72.0 (s). IR (THF, cm^{-1}): ν_{CO} = 2048, 1969, 1950, 1933. IR spectroscopic measurements indicated that a solution of the compound in refluxing THF remained unchanged for 24 h.

Fe(SPh)($Ph_2PC_6H_4CO$)(CO)$_3$, 1. Under a stream of N_2, a solution of Fe(bda)(CO)$_3$ (445 mg, 1.55 mmol) and $Ph_2PC_6H_4C(O)SPh$ (652 mg, 1.63 mmol) in 20 mL of benzene was heated to reflux for 4 h. The solution was evaporated under vacuum and washed with a few milliliters of Et_2O. The brown crystalline solid was dried overnight to give 743 mg of diiron dithiolato complexes. A solution of this mixture (985 mg, 0.992 mmol) in 6 mL of CH_2Cl_2 was stirred under 1600 psi of CO at 60 °C for 24 h to give a near-quantitative conversion to **1**. Pure samples of **1** could be obtained by slow crystallization at −30 °C (see below). For such carbonylations, the solution is first pressurized at 100−500 psi followed by careful venting. This gas-exchange procedure is repeated twice more. The bomb is then pressurized to 1400−1800 psi, with cooling of the bomb as needed to achieve the final pressure. ^{31}P NMR (202 MHz, CD_2Cl_2): δ 72.5. IR (CH_2Cl_2, cm^{-1}): ν_{CO} = 2075, 2025, 2001,1629 (acyl). Single crystals of **1** suitable for X-ray diffraction were obtained by layering hexanes over a solution of 450 mg of **1** in 5 mL of CH_2Cl_2 at −30 °C for 96 h. Orange crystals of **1** were manually separated from a brown unidentified powder.

Fe(SPh)($Ph_2PC_6H_4CO$)(^{13}CO)$_3$, 1^{13}CO. A solution of a mixture of **1** and **2** (8.5 mg, 0.009 mmol, ∼9:1 in favor of **1**) in 1 mL of CH_2Cl_2 in a J-Young NMR tube was frozen, and the tube was evacuated under vacuum. An atmosphere of 0.8 atm of ^{13}CO was introduced, and the tube was sealed. The solution was thawed and analyzed by ^{31}P NMR spectroscopy within 5 min. IR data were obtained within 25 min. ^{31}P NMR (202 MHz, CD_2Cl_2): δ72.0 (d of d of d, $^2J_{CPtrans}$ = 53, $^2J_{CPcis}$ = 21, $^2J_{CPcis}$ = 16 Hz). IR (CH_2Cl_2, cm^{-1}): ν_{CO} = 2027, 1980, 1957, 1629 (acyl).

Et_4N[Fe(SPh)($Ph_2PC_6H_4CO$)(CN)(CO)$_2$], Et_4N[2]. A solution of Et_4NCN (51.6 mg, 0.330 mmol) in 5 mL of CH_2Cl_2 was added to a solution of **1** (164 mg, 0.3304 mmol) in 20 mL of CH_2Cl_2. The solution was stirred 10 min and then concentrated to 2 mL. An oil precipitated upon the addition of 10 mL of Et_2O. The oil was dissolved in THF and reprecipitated by the addition of ether. The resulting oily solid was recrystallized from THF/Et_2O twice more to give an orange tacky solid that converted to an orange powder upon vacuum drying. Yield: 115 mg (52%). ^{31}P NMR (202 MHz, CD_2Cl_2): δ66.73 (s). ESI-MS (negative mode, *m/z*): 536.1 (Calcd for $C_{28}H_{19}FeNO_3PS$: 536.0). IR (CH_2Cl_2, cm^{-1}): $\nu_{CN/CO}$ = 2094 (CN), 2013, 1954, 1597 (acyl). Anal. Calcd for $C_{36}H_{39}FeN_2O_3PS$. Found: C, 64.87 (64.14); H, 5.90 (5.99); N 4.20 (4.33).

Et_4N[Fe(SPh)($Ph_2PC_6H_4CO$)(^{13}CN)(CO)$_2$]. A solution of $Et_4N^{13}CN$ (17 mg, 0.108 mmol) was generated by $K^{13}CN$ and Et_4NCl in MeOH followed by filtration to remove KCl. Solvent was removed by vacuum, and the residue was dissolved in 3 mL of CH_2Cl_2 and added to a solution of **1** (54.0 mg, 0.108 mmol) in 5 mL of CH_2Cl_2. The solution was stirred 10 min and evaporated under vacuum. Upon slurrying in Et_2O, the product converted to an oily orange powder that was dried under vacuum. ^{31}P NMR (202 MHz, CD_2Cl_2): δ66.7, doublet, $^2J_{CP}$ = 24 Hz. IR (CH_2Cl_2, cm^{-1}): ν_{CO} = 2050, 2012, 1954, 1597 (acyl).

Fe(SPh)($Ph_2PC_6H_4CO$)(CO)$_2$(NCCH_2Ts), 3. A solution of **1** (99.6 mg, 0.185 mmol) in 3 mL of CH_2Cl_2 was cooled to −30 °C. A background IR spectrum was recorded in situ. A solution of $TsCH_2NC$ (36.5 mg, 0.185 mmol) in 1 mL of CH_2Cl_2 was added, and IR spectra were collected every minute as the solution was allowed to warm. The CO region of the IR spectra changed cleanly between −10 and −6 °C over the course of ∼30 min. ^{31}P NMR (202 MHz, CD_2Cl_2): δ70.7 (s). IR (CH_2Cl_2, cm^{-1}): $\nu_{CN/CO}$ = 2153 (CN), 2038, 1983, 1615 (acyl). Upon warming the sample above −6 °C, three new ^{31}P NMR signals at δ73.2, 72.6, and 72.2 were

initially observed before many signals appeared at further times. Upon prolonged standing at room temperature, loss of CO was observed.

Protonation of 1. A solution of **1** (30 mg, 0.056 mmol) in 3 mL of CH_2Cl_2 solution cooled to −72 °C was examined by FT-IR spectroscopy to confirm its integrity. A solution of $[H(Et_2O)_2]BAr^F{}_4$ (56.4 mg, 0.056 mmol) in 1 mL of CH_2Cl_2 was added with stirring. Within 5 min the IR spectrum confirmed complete conversion to a new product (IR: 2090, 2041, 2024 cm^{-1}). Addition of Et_3N (10 μL, 0.072 mmol, −72 °C) gave back **1**. The protonated product isomerizes slowly at −30 °C. Protonation was also conducted in a J.Young NMR tube by adding 15.3 mg (0.028 mmol) of **1** and 30.3 mg (0.028 mmol) of $[H(Et_2O)_2]BAr^F{}_4$, followed by vacuum transfer of 0.8 mL of CD_2Cl_2. The sample was warmed to −78 °C and inserted into the NMR probe that had been precooled to −50 °C. The sample was slowly warmed to −30 °C, at which temperature the ^{31}P NMR signal for starting material disappeared and a new signal appeared at δ68.1. The spectrum remained unchanged over the course of 30 min. Upon allowing the sample to warm to 0 °C, no change was noted, but at 20 °C, we observed rapid growth of a new singlet in the ^{31}P NMR spectrum (δ76.7). After 5 min, the signal at δ68.1 had completely disappeared. At longer times at room temperature, many new ^{31}P NMR signals were observed. The resulting solution had an odor of thiol.

XAS Data Collection. In a glovebox, the powder sample (25 μL in volume) was transferred into plastic sample holders covered with polyimide windows, frozen in liquid nitrogen, and kept at 4 K during the experiment. X-ray absorption spectra at the Fe K-edge were recorded in transmission mode at Wiggler station 7-3 (SSRL, Menlo Park, CA) equipped with a Si(220) double-crystal monochromator, a focusing mirror, and a 30-element Ge solid-state fluorescence detector (Canberra). Energy axis of each scan was calibrated by a reference sample (Fe foil). Scan averaging was done with Athena,[46] and normalization and data reduction were performed with the EXPROG[47] using E_0(Fe) = 7120 eV.

XAS Data Analysis. The extended X-ray absorption fine structure (EXAFS) oscillations were analyzed with EXCURV9.2,[48] and the σ^3-weighted spectra were used. Different integer coordination numbers were considered for the ligands CO, CN, C, O, N, P, and S. The fit index was used as a measure of the goodness of the fits. *Ab initio* theoretical phase and amplitude functions were generated within EXCURV. The experimental spectra are compared with the theoretical simulations based on small atom theory. No Fourier filtering was applied. The best model is described in Table 3, and the fit is shown in Figure 3.

Acknowledgment. Research at Illinois was supported by the U.S. Department of Energy - Office of Basic Energy Sciences, grant DE FG01-90er14146 and in part the Petroleum Research Fund. We thank Dr. S. Shima (MPI-Marburg) for helpful advice. The authors are grateful to SSRL for providing beamtime and thank Erik Nelson and colleagues for their excellent support during the beamtime. Portions of this research were carried out at the Stanford Synchrotron Radiation Lightsource, a national user facility operated by Stanford University on behalf of the U.S. Department of Energy, Office of Basic Energy Sciences. The SSRL Structural Molecular Biology Program is supported by the Department of Energy, Office of Biological and Environmental Research, and by the National Institutes of Health, National Center for Research Resources, Biomedical Technology Program.

Supporting Information Available: Crystallographic analysis of **1**; additional spectroscopic and preparative details (including protonation data); reanalysis of EXAFS data for $mHMD^{CN}$ and $mHMD^{CO}$. This material is available free of charge via the Internet at http://pubs.acs.org.

JA1072228

(46) Ravel, B.; Newville, M. *J. Synchrotron Radiat.* **2005**, *12*, 537–541.
(47) Nolting, H.-F.; Hermes, C., *EXPROG*, EMBL EXAFS data analysis and evaluation program package; 1992.
(48) Binsted, N.; Strange, R. W.; Hasnain, S. S. *Biochemistry* **1992**, *31*, 12117–12125.